THE AMERICAN SOCIETY OF MECHANICAL ENGINEERS
345 E. 47th St., New York, N.Y. 10017

96-GT-75

PERFORMANCE BENEFITS FOR WAVE ROTOR-TOPPED GAS TURBINE ENGINES

Scott M. Jones
NASA Lewis Research Center
Aerospace Analysis Office
21000 Brookpark Road, M/S 77-2
Cleveland, Ohio 44135 U.S.A.

Gerard E. Welch
U.S. Army Research Laboratory
Vehicle Propulsion Directorate
21000 Brookpark Road, M/S 77-6
Cleveland, Ohio 44135 U.S.A.

ABSTRACT

The benefits of wave rotor-topping in turboshaft engines, subsonic high-bypass turbofan engines, auxiliary power units, and ground power units are evaluated. The thermodynamic cycle performance is modeled using a one-dimensional steady-state code; wave rotor performance is modeled using one-dimensional design/analysis codes. Design and off-design engine performance is calculated for baseline engines and wave rotor-topped engines, where the wave rotor acts as a high pressure spool. The wave rotor-enhanced engines are shown to have benefits in specific power and specific fuel flow over the baseline engines without increasing turbine inlet temperature. The off-design steady-state behavior of a wave rotor-topped engine is shown to be similar to a conventional engine. Mission studies are performed to quantify aircraft performance benefits for various wave rotor cycle and weight parameters. Gas turbine engine cycles most likely to benefit from wave rotor-topping are identified. Issues of practical integration and the corresponding technical challenges with various engine types are discussed.

NOMENCLATURE

APU = auxiliary power unit
CPR = compressor pressure ratio
GG = gas generator
HPC = high pressure compressor
HPT = high pressure turbine
LPC = low pressure compressor
LPT = low pressure turbine
OPR = overall pressure ratio: (P_3/P_a)
PR = pressure ratio
PR_w = wave rotor pressure ratio: (P_{4A}/P_{3A})
SFC = specific fuel consumption
TOGW = aircraft takeoff gross weight
TR = temperature ratio
TR_w = wave rotor temperature ratio: (T_{4A}/T_{3A}) (also equal to T_{4B}/T_3)
WOPR = wave rotor-topped engine overall pressure ratio: (P_{3B}/P_a)

Cycle station subscripts:
a = ambient conditions
3 = (high pressure) compressor exit
3A = wave rotor inlet port
3B = burner inlet duct
4 = burner outlet duct
4A = wave rotor outlet port
4B = (high pressure) turbine inlet
41 = turbine rotor inlet

INTRODUCTION

The wave rotor is a turbomachine consisting of a rotating annulus divided into axial passages with stationary ducts, or ports, delivering flow to and from the wave rotor (Fig. 1). The number, circumferential location, and thermodynamic conditions of these ports determine the wave rotor cycle. During "steady-state" operation, the flow through the rotating axial passages is alternately exposed to each inlet and outlet port, creating unsteady compression and expansion waves which propagate axially along the passages. Although this wave propagation is unsteady, it is also periodic. This periodic nature allows the wave rotor inlet and outlet flow to remain steady, creating the potential for the wave rotor to be included as part of a steady flow device such as a gas turbine engine. Furthermore, because the wave rotor passages are alternately exposed to hot and cold flows the mean rotor temperature is significantly lower than the peak cycle temperature. This "self-cooling" feature enables topping without increasing the temperature of the flow to the turbines.

The wave rotor is not new; it has been proposed for various applications ranging from stationary power plants to a topping cycle

Presented at the International Gas Turbine and Aeroengine Congress & Exhibition
Birmingham, UK — June 10-13, 1996

for vehicle gas turbine engines. Previous work in this area has been reported by Taussig and Hertzberg (1984), Taussig (1984), and Shreeve and Mathur (1985).

With any new or unconventional technology, cycle and systems studies are the first step in determining the potential impact of that technology on system performance. This paper re-examines wave rotor-topping for gas turbine engines. The benefits of wave rotor-topping for turboshaft engines, subsonic high-bypass turbofan engines, auxiliary power units, and ground power units as well as challenges and risks associated with the various wave rotor applications are discussed. In this work, emphasis is placed on wave rotor performance in the turboshaft and turbofan propulsion systems although the wave rotor may be better suited to other applications.

WAVE ROTOR GENERAL INFORMATION

As mentioned previously, port location and number determine the wave rotor thermodynamic cycle. As shown in Fig. 2, the four-port wave rotor considered here has a port from the compressor (port 3A), a port leading from the wave rotor to the burner (port 3B), a port from the burner back to the wave rotor (port 4), and a port to the turbine (port 4A). This four-port wave rotor cycle is designed to provide a pressure gain with zero net shaft work. The four-port wave rotor is, in theory, easily incorporated into a gas turbine engine with the addition of transition ducts located between the compressor exit and port 3A and between port 4A and the turbine inlet. The two remaining wave rotor ports are connected to the burner. In addition, the performance benefits of a four-port pressure gain cycle are readily quantified for the various applications considered.

A simplified description of how this four-port cycle operates is as follows. The flow from port 3A enters the wave rotor where it is compressed and exits the wave rotor via port 3B. The flow then enters the burner where it is heated to high temperature before re-entering the wave rotor from port 4. Inside the rotor, the flow expands as it compresses the incoming flow. Finally, the flow exits the rotor via port 4A at a higher total pressure and total temperature than it entered the wave rotor. The peak pressure occurs in port 3B and is typically 3-4 times the pressure at port 3A. The peak cycle temperature occurs in port 4 and is 2-3 times the port 3A temperature. However, due to the high rotational speed of the rotor, the axial passages are rapidly exposed to both hot (T_4) and cold (T_{3A}) flows and therefore the rotor assumes a mean temperature significantly less than T_4. This mean temperature is estimated to be close to T_{4A} and allows the wave rotor to top turbine-inlet-temperature-limited cycles.

The primary indicator of the four-port pressure-gain wave rotor performance is PR_w, the ratio of port 4A total pressure to port 3A total pressure. This pressure ratio is primarily a function of the wave rotor temperature ratio (port 4A total temperature to port 3A total temperature, or TR_w). Figure 3 shows the projected wave rotor performance as a function of TR_w. The data in Figure 3 was calculated by Welch, et al., (1995) and assumes values for other wave rotor variables such as mass flow rate and rotor rotational speed. It can be seen that the wave rotor can boost total pressure by 40% with a temperature ratio of about 3.

The wave rotor can be used in conjunction with a burner as part of a gas turbine engine. In this case T_3 is assumed equal to T_{3A}, and T_{4A} is assumed equal to T_{4B}. In such a case, T_{3A} is determined by P_3 or OPR while T_{4A} is equal to the turbine inlet temperature. In order to maximize wave rotor performance (i.e., PR_w) in an engine, then, a low OPR and a high turbine inlet temperature is required for a large TR_w. Historically, the trend in gas turbine engines has been toward rising OPR and T_{41} due to technology and materials advances. Therefore, most gas turbine engines have a temperature ratio T_{4B}/T_3 equal to 1.75-2.25 and a maximum wave rotor pressure ratio between 1.10-1.25 can be expected for these engines.

METHOD OF ANALYSIS

Wave Rotor Analysis

Although wave rotor pressure ratio is heavily dependent upon TR_w, variables specific to the wave rotor design, such as length, rotational speed, number of axial passages, and mass flow rate also affect PR_w due to frictional losses, passage opening and closing losses, and other real-world effects. The design point wave rotor performance is determined from a one-dimensional design/analysis model (Welch, 1996). This model uses mass and energy balances, one-dimensional gas dynamics to model wave processes that effect energy exchange within a passage, and entropy production models to account for losses in boundary layer flows, separated flows, shock waves, and non-uniform port flow field mixing.

Another one-dimensional design/analysis model is used to calculate off-design wave rotor performance. Paxson (1993) has verified this model using experimental data. This model calculates off-design performance by solving the unsteady viscous flow field in an axial passage for time-constant inlet and outlet port conditions. The model accounts for losses due to gradual passage opening (and closing), viscous effects, heat transfer effects, leakage, and non-uniform port flow field mixing. The output of the code is used to create a wave rotor operating "map". This map is a table of PR_w as a function of off-design values of wave rotor RPM, wave rotor mass flow rate, and heat addition in the burner. Both the design point and off-design models include the burner pressure drop as part of the wave rotor performance calculation.

In some cases the wave rotor performance is "penalized". Typically, gas turbine engines use high pressure compressor bleed flow for turbine cooling. In wave rotor-topped cycles the turbine inlet total pressure is higher than the compressor exit total pressure ($P_{4B} > P_3$), and the peak cycle pressure occurs within the wave rotor. This means that in order to cool the first turbine stage, flow must be taken from a high pressure port of the wave rotor (port 3B in this case). Since this bleed flow is no longer available to do work in the remaining part of the wave rotor, the overall wave rotor performance is reduced or "penalized". The amount of the performance drop is proportional to the percentage of bleed flow required. Figure 4 shows the percentage decrease in wave rotor pressure gain as a function of the amount of compressor flow required for turbine cooling. The graph shows that a cooling flow of 20%, not uncommon in modern gas turbines, reduces wave rotor pressure gain by approximately 50% (e.g. PR_w goes from 1.20 to 1.10). In addition, wave rotors with lower performance appear to be slightly more sensitive to removing flow from the wave rotor as shown by the steeper slopes for the lower TR_w cycles.

Cycle Analysis

The cycle performance is calculated using a one-dimensional steady-state thermodynamic cycle analysis code. The NASA Engine Performance Program (NEPP) allows the user to model virtually any kind of gas turbine engine cycle through the use of components which can be placed in any order to create the desired cycle (Klann and Snyder, 1994). For this study, a new component subroutine was added to NEPP. This new subroutine models the wave rotor component as a combination of a wave rotor and a burner, similar to that shown in Fig. 2. The wave rotor component has only one inlet flow station (station 3A) and one outlet flow station (station 4A) and therefore acts similar to a burner with a pressure gain. Because the wave rotor component in NEPP has only one inlet and one outlet flow station, it does not have allowance for bleed flow in its configuration. Because some of the study engines require cooling, the cooling flow for the wave rotor-topped engines is taken from the compressor (just as it is for the baseline engines), but the cooling-penalized wave rotor performance is used. This creates a slight error as the enthalpy of the cooling flow is lower than it would be if it were taken from the wave rotor.

In order to determine the benefit of wave rotor-topping, a baseline engine type along with representative cycle parameters is chosen and modeled. Once the baseline engine has been created, the wave rotor-enhanced engine model is created by replacing the burner component of the baseline cycle with the wave rotor component. Care is taken to make sure all the other component inputs are unchanged whenever possible. In order for reasonable performance comparisons to be made, the turbine inlet temperature (T_{4B}) and OPR of the enhanced engine are kept the same as the baseline unless stated otherwise. In addition, pressure drops of 2% are added to the duct components immediately fore and aft of the wave rotor. These pressure drops account for the transition ducts that go from the compressor exit to port 3A and from port 4A to the turbine inlet. For the wave rotor-enhanced cycles, the burner pressure drop is accounted for in the wave rotor pressure ratio and is greater than the burner pressure drop of the baseline.

Engine Weight and Aircraft Gross Weight Analysis

The weight and dimensions of the turbofan engines is estimated by the WATE code (Onat and Klees, 1979). This code has been considerably enhanced from its original version. Using key component design variables in a preliminary design approach, the WATE code determines the weight of each engine component. The overall estimated engine weight is accurate to 5%. The weight of the wave rotor component is not calculated by the WATE code. A rough calculation of the weight of the wave rotor for the turbofan application is made based on estimated thickness of the rotor casing, rotor materials, and required ducting.

The aircraft mission and sizing analysis is performed by the Flight Optimization System (FLOPS) code, which uses as inputs the engine performance data, a mission profile, and aircraft description including weights, aerodynamics, and geometry (McCullers, 1984). The aircraft model and mission used for this study is similar to the Boeing 777 subsonic transport aircraft. The mission profile consists mainly of a climb to 33000 ft (10000 m) at Mach 0.83, a best-Breguet-altitude cruise, and a descent with a total aircraft range of 6500 nm (12000 km). The aircraft carries 300 passengers and requires two engines rated at about 90000 lbs (400 kN) thrust each. For this study the aircraft wing loading and the aircraft thrust-to-weight are kept constant rather than perform an aircraft sizing thumbprint for each engine and weight variation.

RESULTS AND DISCUSSION

Turboshaft Engines

Schematics of the baseline and the wave rotor-topped turboshaft configurations are shown in Fig. 5. The baseline engine consists of a conventional gas generator (compressor, burner, and turbine) on one shaft and a power turbine on a separate shaft. The wave rotor-topped turboshaft replaces the burner component with the wave rotor/burner component. Figure 6 shows the increase in design point shaft power possible for wave rotor-enhanced turboshaft engines of varying compressor pressure ratio and T_{4B}. The wave rotor pressure ratio for each engine is determined from the curve in Fig. 3 and varies from PR_w=1.095 for the CPR=50, T_{4B}=2880 R (1600 K) design to a PR_w=1.500 for the CPR=5, T_{4B}=3240 R (1800 K) design. The mass flow for all the engines is 22 lb/s (10 kg/s), but the results are qualitatively applicable to turboshafts of any mass flow. For a given T_{4B}, increasing compressor efficiency has a very small beneficial effect due to the resultant decrease in T_3 and subsequent increase in TR_w. As expected, the engines with the lowest CPR and highest T_{4B} receive the highest benefit from wave rotor-topping due to their higher wave rotor pressure ratios. These results assume no cooling flow taken from the wave rotor. Because turbine cooling is generally required for turbine inlet temperatures exceeding approximately 2160 R (1200 K), these enhanced engines will have to rely on some unconventional cooling scheme in order to achieve the performance benefits shown. This scheme could be an additional compressor to pressurize only the cooling flow or a cooling method that does not require the cooling flow pressure to be higher than the turbine inlet pressure.

Should cooling flow be taken from the wave rotor, the PR_w (and subsequent cycle performance benefit) suffers. In addition, if this extracted bleed flow is at a higher temperature than the compressor discharge flow (as is the case with port 3B flow) then the coolant bleed fraction must be increased. Figure 7 shows the design point decrease in shaft power of baseline and wave rotor-enhanced turboshaft engines with parametrically varying cooling flow. The baseline and wave rotor-topped engines have a CPR=8, T_{4B}=2390 R (1325 K), and a mass flow rate of 5.0 lb/s (2.3 kg/s). Also shown (by the arrows) are the wave rotor-enhanced equivalent cooling percentages for the given baseline cooling percentages. The equivalent cooling percentage is based on the enthalpy of the peak pressure flow in wave rotor port 3B as this is where the cooling flow is most likely to be obtained for this four-port design. It can be seen that a baseline engine with 15% cooling flow has a shaft power of 514 HP (383 kW), while the corresponding wave rotor engine requires almost 20% of the higher temperature cooling flow to maintain the same turbine blade temperature and has 571 HP (426 kW). As seen in the graph, the wave rotor-topped engines rapidly lose any performance benefit once the baseline cooling flow exceeds 20% due to the higher cooling flows required and the corresponding lower wave rotor pressure ratios.

The off-design performance benefit of wave rotor-topping is calculated using a turboshaft with 5% cooling flow as a baseline. The engine parameters are the same as those in Figure 7 and are listed in

Table 1. This baseline engine is similar to small turboshaft engines which are primarily used in helicopter applications. Table 2 lists the performance data for the baseline and wave rotor turboshafts. At design the baseline engine is capable of delivering 599 HP (447 kW) and has a temperature ratio of 2.21. The wave rotor designed for this engine has a pressure ratio of 1.24 without considering the penalty for cooling flow taken from the wave rotor. For a bleed flow of 5%, the wave rotor pressure ratio falls to 1.21 but, as Fig. 7 shows, the wave rotor engine needs 7% bleed when coolant is taken from port 3B which reduces PR_w to 1.20. At design, the wave rotor-enhanced turboshaft produces 709 HP (529 kW), or 18% more than the baseline. Both engines are run off-design to approximately 40% of maximum shaft power, and Figure 8 shows the specific fuel consumption and shaft power for the baseline and wave rotor-topped turboshafts. The graph shows that at off-design the wave rotor-topped turboshaft behaves similar to the baseline; i.e., the SFC curves for the wave rotor engine and the untopped engine show the same trends. The off-design wave rotor pressure ratio decreases as the engine power and temperature is decreased. For the wave rotor-topped engine at 84.5% power (comparable to the baseline engine full power), the wave rotor pressure ratio and fuel flow are 1.19 and 312 lb/hr (142 kg/hr), respectively. The inlet flow and T_{4B} are 4.74 lb/s (2.15 kg/s) and 2296 R (1276 K), respectively, at this point. In other words, for the same shaft power the wave rotor-enhanced engine has 13% less fuel flow, a T_{4B} 94 R (52 K) cooler, and 6% lower air flow.

Auxiliary Power Units

Auxiliary power units are essentially a type of turboshaft engine. Rather than supply shaft power to a propeller, APU's for aircraft applications are typically used to supply both pressurized air to aircraft pneumatic and environmental control systems as well as supply shaft power to an electrical generator (Hoose, 1983). Other APU's, sometimes called small power units, are used to supply shaft power for various applications ranging from helicopter and tank engine starting to generators for mobile power systems.

APU's tend to have small mass flows (7 lb/s or less), low OPR's (around 4), and little if any turbine cooling. This makes them good candidates for wave rotor enhancement. Two cycle models are used to determine the benefits of wave rotor-topping of auxiliary power units. The first model uses the wave rotor as a high pressure spool in the engine core like the turboshaft engines previously discussed. The second model uses the wave rotor to replace the compressor and burner components of the APU. Figure 9 shows the schematics of the baseline and wave rotor-enhanced APU configurations.

The baseline APU cycle is of the integral bleed type. As shown in Tables 3 and 4, this APU is designed to supply 1.71 lb/s (0.775 kg/s, or 28% of the compressor exit air) at 51 psia (352 kPa) to the pneumatic systems while the turbine supplies power for the compressor and an additional 60 HP (45 kW) to run a generator. It has no cooling flow. Table 4 shows the performance data for the baseline and the wave rotor-topped auxiliary power units. Due to the low OPR of APU engines, the addition of the wave rotor increases shaft power immensely; for this cycle, the wave rotor-topped APU supplies 212% more shaft power than the baseline. Indeed, for many gas turbine cycles representative of auxiliary power units, the wave rotor-enhanced engines can easily double the available shaft power! Alternatively the wave rotor APU can be designed for the same shaft power, bleed mass flow, and bleed pressure as the baseline. Such an APU has 17% less intake mass flow than the baseline. Even with such substantial improvements, however, the additional weight and complexity of the wave rotor may overshadow the performance gain for this configuration.

The second wave rotor APU design consists only of the wave rotor (with burner) and a power turbine. The bleed air is taken from port 3B and is at roughly 55 psia (380 kPa). Ordinarily the wave rotor pressure ratio could be as high as 1.5 for this TR_w, but the high amount of bleed flow reduces PR_w to about 1.24. However, this small pressure gain is enough for the power turbine to extract the 60 HP (45 kW) needed to run the electrical generator. The wave rotor APU should weigh significantly less than the wave rotor-topped APU as the compressor component has been removed and the turbine has a much smaller expansion ratio. The disadvantage is that the fuel flow is 60% higher and the turbine corrected flow has substantially increased. Although it was not considered here, it is possible to design a wave rotor to provide shaft power instead of a pressure gain (i.e., a wave engine). Such a design may make it possible to remove the turbine from the APU cycle as well. Such an APU would consist only of a wave rotor/burner which has bleed taken from one duct and a shaft leading to a generator. Although its fuel consumption would be higher, this type of wave rotor APU has the potential for improvements in weight, manufacturing cost, and reliability and maintainability over a conventional auxiliary power unit.

Ground Power Units

Many ground power plants use gas turbine engines to supply shaft power to electrical generators. These ground power units are often turboshaft engines originally developed as aircraft powerplants. These engines are typically de-rated to extend their service time to the long hours necessary for economical operation (Cohen, et al., 1987). For these ground power units, the wave rotor can be used as a topping cycle similar to the turboshafts discussed previously. Tables 5 and 6 list the cycle and performance data for the baseline and wave rotor-enhanced ground power units. For the first cycle, the wave rotor pressure ratio is 1.20 and its addition increases the shaft power by 14%. Alternatively, the wave rotor-topped ground power unit can supply the same power as the baseline with turbine inlet temperature reduced by 103 R (57 K), reducing fuel consumption by 10%. This reduction in T_{4B} significantly extends the useful life of the hot section components. In addition, with ground power plants it is assumed weight and size are not major factors. The wave rotor still adds complexity to the overall engine, however.

Turbofan Engines

For the turbofan engine, a baseline cycle representative of a current technology subsonic high-bypass separate-flow turbofan is chosen. The OPR and T_{4B} are 39 and 3200 R (1778 K), respectively, for this cycle. Table 7 lists the values of the major design point variables. The wave rotor-enhanced turbofan uses the wave rotor pressure gain to increase engine thrust while keeping fuel flow constant relative to the baseline. Figure 10 is a schematic of the baseline and wave rotor turbofans. For the enhanced turbofan, the on-design wave rotor pressure ratio is 1.08. This value takes into

account the 20% cooling flow typical of modern turbofan engines. Note that for the four-port wave rotor design, the wave rotor turbofan requires a larger amount of cooling than the baseline for the same reason as the turboshaft engine discussed above. Preliminary studies indicate that for this turbofan cycle the cooling flow taken from the wave rotor port 3B is too high in temperature to be effectively used for turbine cooling. Therefore it is assumed that the wave rotor cooling flow is at the same temperature as the baseline cooling flow. This assumption is reasonable if a wave rotor cycle can be designed to provide cooling air at a pressure just above P_{4B} with a temperature close to T_3. A preliminary analysis of a five-port wave rotor design shows that this is feasible.

Table 8 lists the performance data for the turbofan cycles. The wave rotor-topped turbofan has its thrust increased by 2% at design by the wave rotor and its SFC is similarly decreased. The corrected flow into the high-pressure and low-pressure turbines is reduced by the increase in pressure created by the wave rotor and this has several effects. First, the weights of the HPT and LPT are decreased by 6% and 10%, respectively; this translates into a 2-3% reduction in total engine weight. Second, the smaller turbine areas reduce the value of AN^2 (which is proportional to blade pull stress) in both turbines by 8%. It is difficult to predict the weight of the wave rotor due to its extreme pressures and temperatures and their unsteady nature. A preliminary weight calculation for this application indicates that the wave rotor and ducting weight (excluding the burner) is approximately 1650 lb (750 kg, or 25% of the baseline turbofan core weight).

The baseline and wave rotor-topped engines are run off-design for an envelope of altitudes and Mach numbers not exceeding M=0.85 and 40000 ft (12000 m) with several engine throttle curves calculated at discrete Mach numbers and altitudes. This engine deck is used by the mission analysis code to interpolate engine performance at any Mach number, altitude, and throttle setting for the entire aircraft mission. For the wave rotor-enhanced turbofan, two cycle decks are created. The first has a PR_w=1.08, which is the predicted value based on the current analysis. The second cycle deck has a PR_w=1.15 which is chosen to show the aircraft TOGW sensitivity to increased wave rotor performance. This higher performance is attainable if the cooling flow is not taken from the wave rotor (e.g. the HPC flow is pressurized further and used for cooling). The baseline turbofan results in an aircraft takeoff gross weight equal to 588000 lb (267000 kg). Because the weight of the wave rotor is not precisely known, Figure 11 shows the relative TOGW of the aircraft with the wave rotor-topped turbofans as a function of the wave rotor weight. The addition of the wave rotor with a PR_w of 1.08 reduces TOGW 2-5% depending on wave rotor weight. The higher performance wave rotor reduces aircraft TOGW an additional 3%.

A variant turbofan cycle uses the wave rotor to replace stages of the high pressure compressor where the pressure gain from the wave rotor offsets the reduction in HPC pressure ratio. The thrust, SFC, and amount of turbine cooling of the wave rotor-enhanced turbofan cycle are kept the same as the baseline. Unfortunately, the wave rotor pressure ratio is so small that only the last stage of the 10-stage HPC can be removed. The turbine inlet temperature is lowered 41 R (23 K) and the HPC pressure ratio is reduced from 15.8 to 14.2 for the wave rotor-topped turbofan. It is apparent that using the wave rotor to reduce the HPC pressure ratio will produce a significant weight penalty, but the lower T_{4i} will extend the life of the turbine components and may allow for lesser turbine cooling.

Practical Integration and Technical Challenges

There are a number of challenges presented by integrating a wave rotor with a gas turbine engine. Transition ducts which connect the annular flow compressor and turbine to the partial-annulus ports have to be carefully designed to avoid flow separation and high pressure losses; similarly, the ducts to and from the burner with their 180-degree turns must be designed to avoid severe pressure losses. In general, though, the design of these ducts is far from insurmountable. Furthermore, extraction of bleed flow from the wave rotor for turbine cooling should not add much complexity although it will decrease wave rotor performance.

There are other technical issues that have to be addressed. The wave rotor will require tight clearances to prevent leakage between the axial passages and the wave rotor end walls. Also, some mechanism must be used to maintain and regulate wave rotor rotational speed. Fortunately, it is expected that a wave rotor will have a rapid and stabilizing response to transient flow conditions, alleviating compressor surge in a topped engine (Taussig and Hertzberg, 1984). Some wave rotor designs have multiple cycles for each rotor revolution. These multiple cycles allow greater flexibility in design, but synchronization of each cycle may be a problem along with the increase in complexity from multiple ducts. Combustion inside the wave rotor axial passages is being studied (Nalim, 1995) in order to eliminate the separate burner, but the effect combustion-on-the-rotor has on variables such as fuel mixing, atomization, and ignition is not yet fully known.

Engines with high turbine inlet temperatures present the biggest challenge to practical implementation of a four-port wave rotor. These high T_{4i} cycles must supply cooling air to the turbines and, if the temperature is high enough, to the wave rotor as well. The wave rotor engines in this study have a T_4 about 20% greater than the turbine inlet temperature, potentially requiring ceramics or other high temperature, high pressure materials in burner and outlet duct manufacture. If the wave rotor must supply cooling air to the turbines it will likely be taken from port 3B, where the temperature is approximately 25% greater than T_3. Cycles with high T_3's (and T_{3B}'s) can therefore require excessive and impractical amounts of cooling flow and the wave rotor pressure ratio then becomes almost negligible. The average rotor temperature is estimated to be approximately equal to the turbine inlet temperature, which means that the rotor itself could require cooling. The stresses in the wave rotor may be low enough, however, to allow for ceramics in its manufacture which could increase the allowable rotor temperature. Lastly, the peak pressure in the wave rotor is about 2.5-3.5 times P_3; for modern engines this means WOPR's greater than 100 and potentially large weight penalties for designs strong enough to withstand such pressures.

SUMMARY AND CONCLUSIONS

The wave rotor is a proven technology. Cycle analysis has shown that a wave rotor can increase performance of practically any type of gas turbine engine. The amount wave rotor-topping increases performance depends not only on engine type but on engine specific

design variables, primarily OPR, T_{41}, and the amount of cooling flow. Wave rotor performance is reduced when cooling flow is taken from the wave rotor, and wave rotor-topping is impractical for engines which require large (20% or higher) amounts of cooling flow to be extracted from the wave rotor itself. The wave rotor should be considered for individual applications on an engine specific basis.

Detailed studies are certainly in order to fully explore the potential of the wave rotor as part of an auxiliary power unit or turboshaft with low amounts of cooling flow. These studies should include the following: a) a detailed performance analysis of various wave rotor designs (e.g., a 5-port cycle) with an aim toward optimizing *system* performance realizing cooling flow may be required from the wave rotor; b) an analysis to calculate rotor stresses, weight, and temperature; c) a rotational speed analysis to determine how to regulate wave rotor speed; and d) a design (perhaps using CFD) of transition ducts to determine their pressure losses, flow characteristics, and their corresponding impact on turbine and wave rotor system performance.

REFERENCES

Cohen, H., Rogers, G. F. C., and Saravanamuttoo, H. I. H., 1987, *Gas Turbine Theory*, 3rd Edition, Longman Scientific and Technical with John Wiley and Sons, Inc., New York, NY, pp. 17-22.

Hoose, W., 1983, "APU Operational Efficiency," *AGARD Conference Proceedings No. 352, Auxiliary Power Systems*, pp. 13- 1-15.

Klann, J. L., and Snyder, C. A., 1994, "NEPP Programmers Manual (NASA Engine Performance Program)," Vols. I and II, NASA Technical Memorandum 106575, NASA Lewis Research Center, Cleveland, OH.

McCullers, L., 1984, "Aircraft Configuration Optimization Including Optimized Flight Profiles," *Proceedings of the Symposium on Recent Experiences in Multidisciplinary Analysis and Optimization*, NASA CP 2327.

Nalim, M. R., 1995, "Preliminary Assessment of Combustion Modes for Internal Combustion Wave Rotors," NASA Technical Memorandum 107000, NASA Lewis Research Center, Cleveland, OH. (Also AIAA-95-2801)

Onat, E., and Klees, G. W., 1979, "A Method to Estimate Weight and Dimensions of Large and Small Gas Turbine Engines," NASA CR 159481.

Paxson, D. E., 1993, "A Comparison Between Numerically Modeled and Experimentally Measured Loss Mechanisms in Wave Rotors," NASA Technical Memorandum 106279, NASA Lewis Research Center, Cleveland, OH. (Also AIAA-93-2522)

Shreeve, R. P., and Mathur, A. (editors), 1985, *Proceedings of the 1985 ONR/NAVAIR Wave Rotor Research and Technology Workshop*, Report # NPS-67-85-008, Naval Postgraduate School, Monterey, CA

Taussig, R., and Hertzberg, A., 1984, "Wave Rotors for Turbomachinery," ed. Sladky, J. F., Jr., *Machinery for Direct Fluid - Fluid Energy Exchange*, AD-07, The American Society of Mechanical Engineers, New York, NY, pp 1-7.

Taussig, R. T., 1984, "Wave Rotor Turbofan Engines for Aircraft," ed. Sladky, J. F., Jr., *Machinery for Direct Fluid - Fluid Energy Exchange*, AD-07, The American Society of Mechanical Engineers, New York, NY, pp 9-45.

Welch, G. E., 1996, "Macroscopic Balance Model for Wave Rotors," NASA Technical Memorandum 107114, NASA Lewis Research Center, Cleveland, OH. (Also AIAA-96-0243)

Welch, G. E., Jones, S. M., and Paxson, D. E., 1995, "Wave Rotor-Enhanced Gas Turbine Engines," NASA Technical Memorandum 106998, NASA Lewis Research Center, Cleveland, OH. (Also AIAA-95-2799)

TABLE 1: Turboshaft Cycle Parameters

	Baseline Turboshaft Design Point	Wave Rotor Turboshaft Design Point	Wave Rotor Turboshaft Off-design, 85% power
inlet flow	5.03 lb/s (2.28 kg/s)	5.03 lb/s (2.28 kg/s)	4.74 lb/s (2.15 kg/s)
inlet recovery	1.00	1.00	1.00
inlet temperature	549.7 R (305 K)	549.7 R (305 K)	549.7 (305 K)
compressor PR	7.77	7.77	7.21
compressor efficiency	0.81	0.81	0.80
compressor corrected flow	5.18 lb/s (2.35 kg/s)	5.18 lb/s (2.35 kg/s)	4.88 lb/s (2.21 kg/s)
cooling flow, %	5.0[a]	6.9[b]	6.9[b]
wave rotor TR	-	2.21	2.17
turbine inlet temperature	2390 R (1328 K)	2390 R (1328 K)	2296 R (1276 K)
GG turbine efficiency	0.86	0.86	0.86
power turbine efficiency	0.86	0.86	0.86

[a] : cooling flow at compressor exit temperature
[b] : cooling flow at port 3B temperature

TABLE 2: Turboshaft Performance Results

	Baseline Turboshaft Design Point	Wave Rotor Turboshaft Design Point	Wave Rotor Turboshaft Off-design, 85% power
wave rotor PR	-	1.20	1.19
GG turbine expansion ratio	2.87	2.88	2.86
GG turbine corrected flow	1.45 lb/s (0.66 kg/s)	1.19 lb/s (0.54 kg/s)	1.19 lb/s (0.54 kg/s)
power turbine expansion ratio	2.30	2.75	2.56
power turbine corrected flow	3.92 lb/s (1.78 kg/s)	3.28 lb/s (1.49 kg/s)	3.26 lb/s (1.48 kg/s)
Shaft power	599 HP (447 kW)	709 HP (529 kW)	600 HP (447 kW)
Fuel flow	357 lb/hr (162 kg/hr)	354 lb/hr (161 kg/hr)	312 lb/hr (142 kg/hr)
Specific fuel consumption	0.596 lb/hr/HP (0.362 kg/hr/kW)	0.499 lb/hr/HP (0.304 kg/hr/kW)	0.521 lb/hr/HP (0.318 kg/hr/kW)

TABLE 3: Auxiliary Power Unit Cycle Parameters

	Baseline APU	Wave Rotor APU Topped Cycle	Wave Rotor APU No Compressor
inlet flow	6.02 lb/s (2.73 kg/s)		
inlet recovery	1.00		
inlet temperature	559.7 R (311 K)		
compressor PR	4.0	4.0	-
compressor efficiency	0.77	0.77	-
compressor corrected flow	6.25 lb/s (2.83 kg/s)	6.25 lb/s (2.83 kg/s)	-
bleed flow, %	28.4		
Bleed flow rate	1.71 lb/s (0.775 kg/s)		
wave rotor TR	-	2.30	3.73
turbine inlet temperature	2086 R (1159 K)	2086 R (1159 K)	2085 R (1158 K)
turbine efficiency	0.83		

TABLE 4: Auxiliary Power Unit Performance Results

	Baseline APU	Wave Rotor APU Topped Cycle	Wave Rotor APU No Compressor
wave rotor PR	-	1.25	1.24
turbine expansion ratio	3.26	4.13	1.09
turbine corrected flow	2.34 lb/s (1.06 kg/s)	1.83 lb/s (0.83 kg/s)	7.27 lb/s (3.30 kg/s)
Shaft power	60.0 HP (44.7 kW)	187 HP (139.4 kW)	60.0 HP (44.7 kW)
Fuel flow	281 lb/hr (127 kg/hr)	281 lb/hr (127 kg/hr)	449 lb/hr (204 kg/hr)
Bleed flow pressure	51.0 psia (352 kPa)	51.0 psia (352 kPa)	54.8 psia (378 kPa)

TABLE 5: Ground Power Unit Cycle Parameters

	Baseline Ground Power Plant	Wave Rotor Ground Power Plant - Design A	Wave Rotor Ground Power Plant - Design B
inlet flow	220 lb/s (100 kg/s)		
compressor pressure ratio	10.0		
compressor efficiency	0.84		
cooling flow, %	1.0		
wave rotor TR	-	2.08	1.98
turbine inlet temperature	2250 R (1250 K)	2250 R (1250 K)	2147 R (1193 K)
GG turbine efficiency	0.90		
Power turbine efficiency	0.91		

TABLE 6: Ground Power Unit Performance Results

	Baseline Ground Power Plant	Wave Rotor Ground Power Plant - Design A	Wave Rotor Ground Power Plant - Design B
wave rotor PR	-	1.20	1.17
GG turbine expansion ratio	3.06	3.06	3.27
Power turbine exp, ratio	3.04	3.66	3.33
Shaft power	33550 HP (25.0 MW)	38210 HP (28.5 MW)	33550 HP (25.0 MW)
Fuel flow	14220 lb/hr (6450 kg/hr)	14220 lb/hr (6450 kg/hr)	12840 lb/hr (5820 kg/hr)

TABLE 7: Turbofan Cycle Parameters

Design Variable	Baseline Engine	Wave Rotor Engine Design A: PR_w=1.08	Wave Rotor Engine Design B: PR_w=1.15
inlet flow	2800 lb/s (1270 kg/s)		
inlet recovery	1.00		
inlet temperature	545.7 R (303 K)		
bypass ratio	7.00		
fan PR	1.59		
fan efficiency	0.91		
fan corrected flow	2875 lb/s (1304 kg/s)		
LPC PR	1.55		
LPC efficiency	0.88		
HPC PR	15.8		
HPC efficiency	0.85		
HPT inlet temp.	3200 R (1778 K)		
bleed flow, %	19.5		
wave rotor TR	1.91		
HPT efficiency	0.89		
LPT efficiency	0.93		

TABLE 8: Turbofan Performance Results

	Baseline Engine	Wave Rotor Engine Design A: PR_w=1.08	Wave Rotor Engine Design B: PR_w=1.15
wave rotor PR	-	1.08	1.15
HPT expansion ratio	4.87	4.87	4.87
HPT corrected flow	19.8 lb/s (8.98 kg/s)	18.2 lb/s (8.26 kg/s)	17.0 lb/s (7.71 kg/s)
LPT expansion ratio	5.15	5.15	5.15
LPT corrected flow	96.0 lb/s (43.5 kg/s)	87.9 lb/s (39.9 kg/s)	82.1 lb/s (37.2 kg/s)
Net thrust	86820 lb (386 kN)	88370 lb (393 kN)	89470 lb (398 kN)
SFC	0.313 lb/hr/lb 0.0319 kg/hr/N	0.308 lb/hr/lb 0.0314 kg/hr/N	0.304 lb/hr/lb 0.0310 kg/hr/N
Engine weight	20430 lb (90.9 kN)	19990 lb + wave rotor (88.9 kN) + wave rotor	19470 lb + wave rotor (86.6 kN) + wave rotor

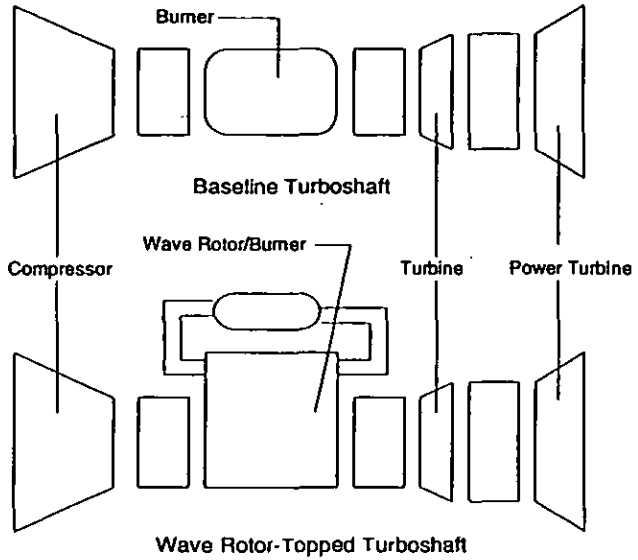

Figure 5: Baseline and Wave Rotor-Topped Turboshaft Schematic Diagrams

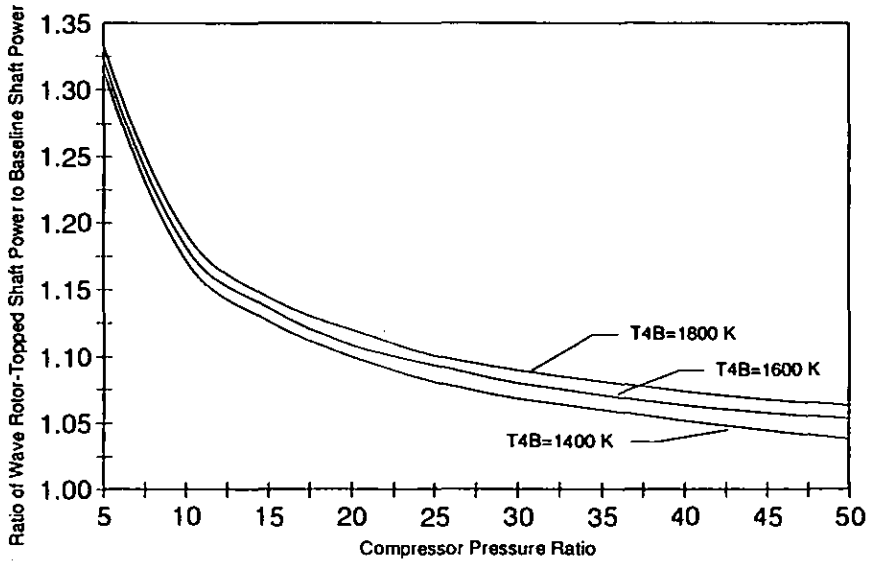

Figure 6: Wave Rotor Shaft Power Benefit for Turboshafts of Varying CPR and T4B

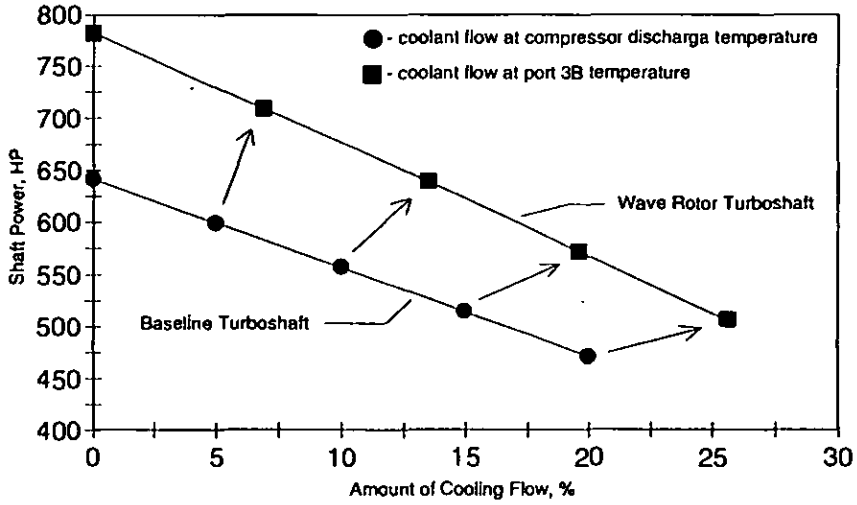

Figure 7: Design Point Shaft Power for Baseline and Wave Rotor-Topped Turboshafts as a Function of Required Cooling Flow

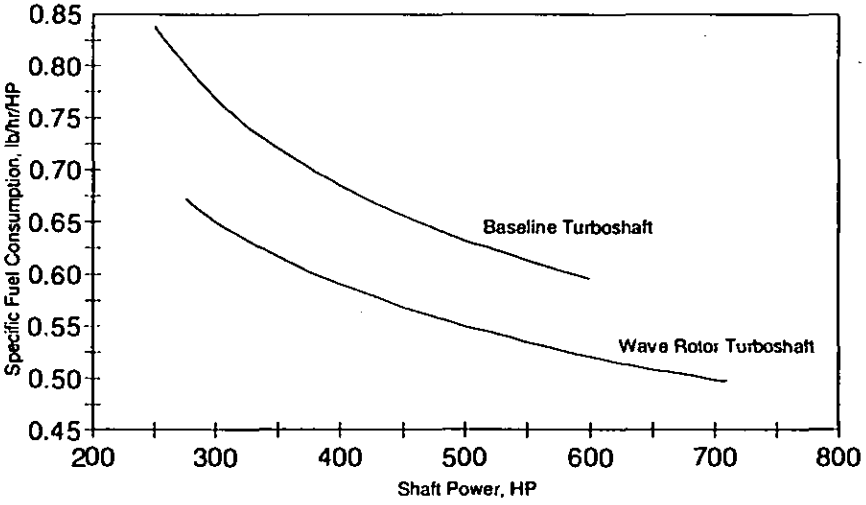

Figure 8: Off-Design Performance Benefit for Wave Rotor-Topped Turboshaft Engine

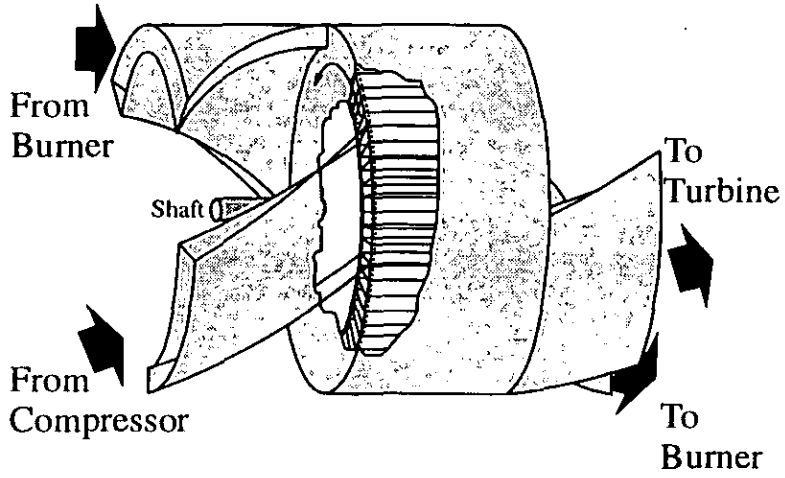

Figure 1: Four-port Wave Rotor Schematic Diagram

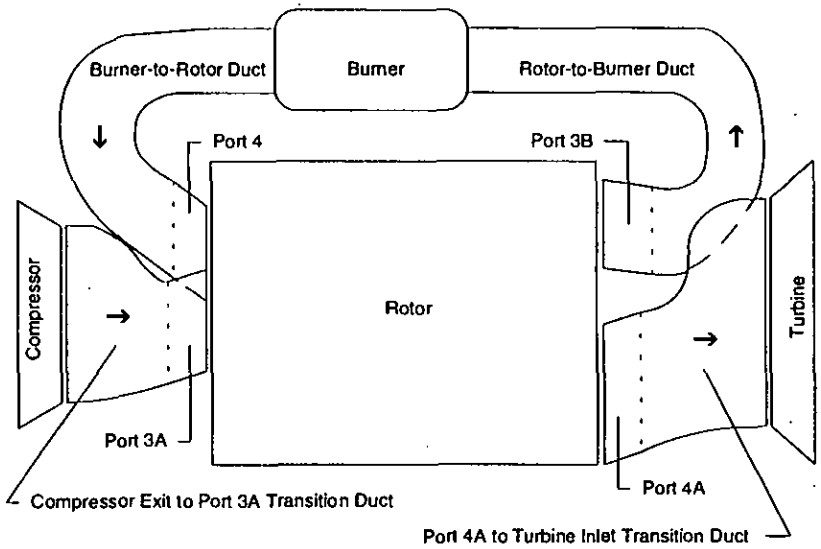

Figure 2: Wave Rotor and Burner Schematic Diagram

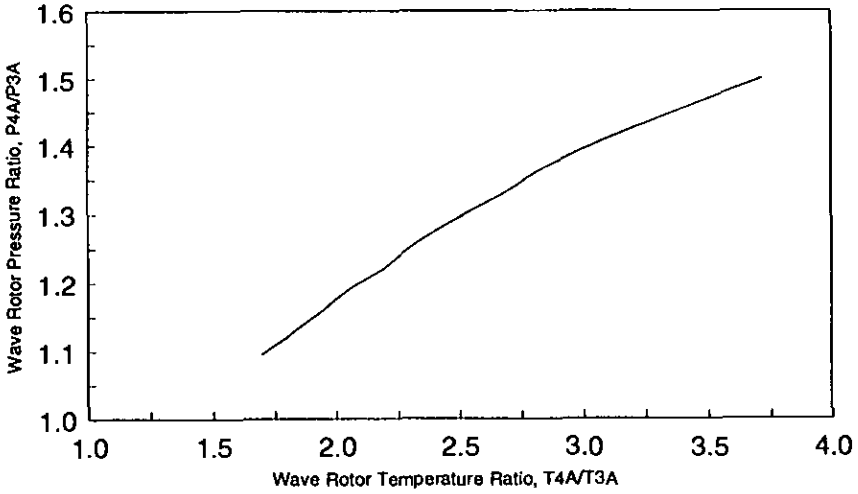

Figure 3: Design Point Wave Rotor Pressure Ratio

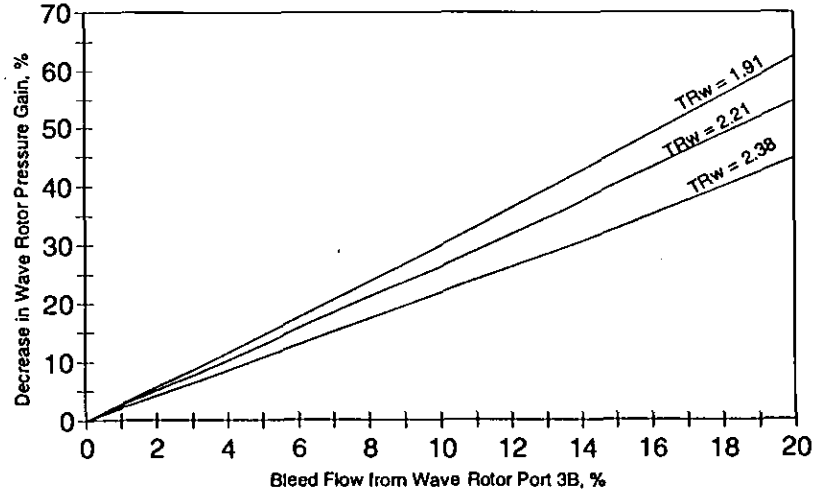

Figure 4: Decrease in Wave Rotor Pressure Gain as a Function of Bleed

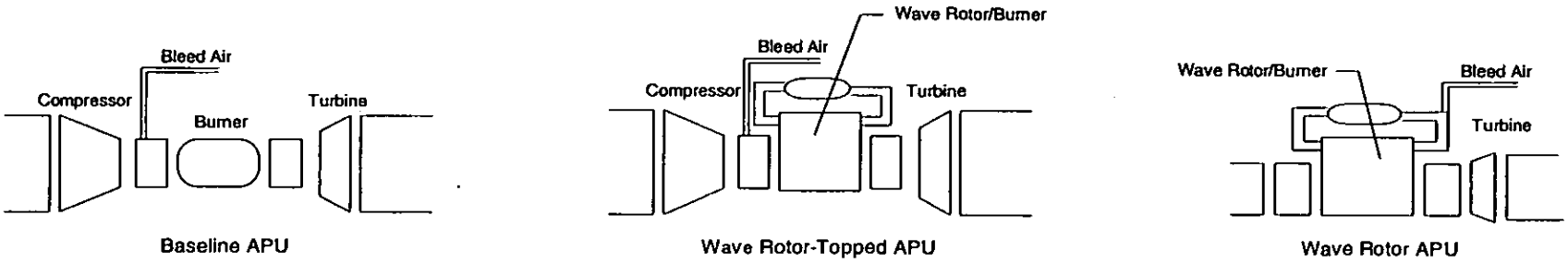

Figure 9: Auxiliary Power Unit Schematic Diagrams

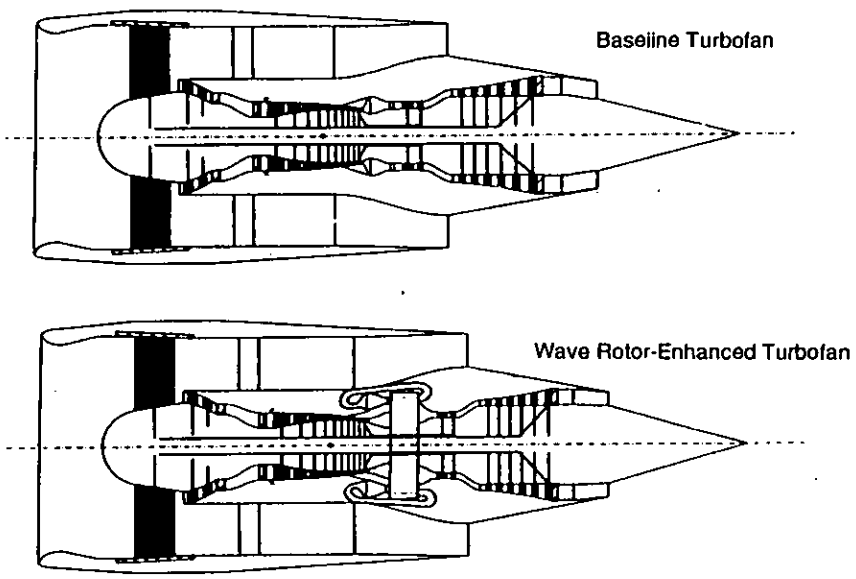

Figure 10: Baseline and Wave Rotor-Topped Turbofan Schematic Diagrams

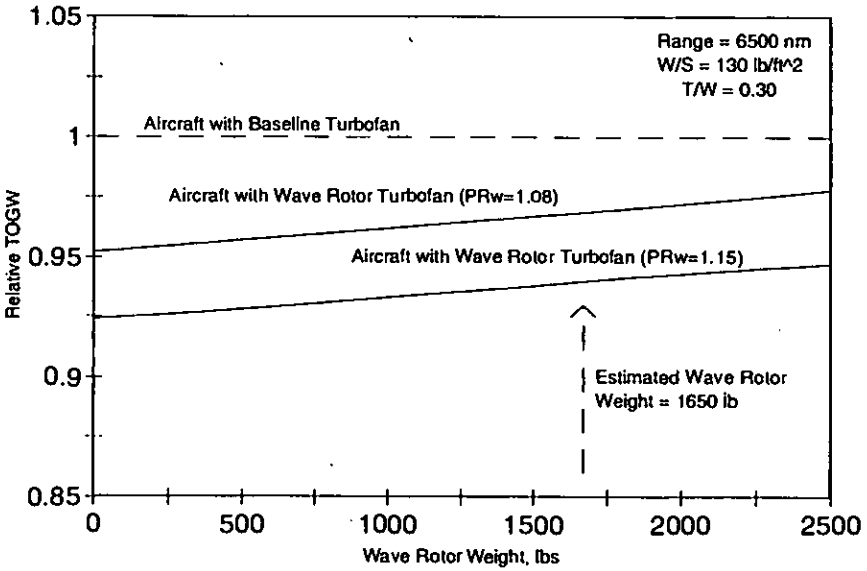

Figure 11: TOGW Benefit for a Subsonic Transport with a Wave Rotor-Topped Turbofan